Real-time breast deformation using non-linear tissue properties

Markus T. Harz[1], Joachim Georgii, Kathy Schilling, and Horst K. Hahn

[1]markus.harz@mevis.fraunhofer.de

Abstract: Localization of target structures in open surgical breast procedures mostly relies on localization wires that give coarse orientation hints together with a set of radiological images to convey the extent and location. Patient positioning, however, is different for image acquisition and surgery. We propose to simulate the breast deformation between these positions to track and visualize the target position. To date no sufficiently fast and accurate methods have been proposed for that purpose, which is caused by the computational expensiveness caused by the non-linear behavior of the material. In contrary, the efficient FEM-based simulation framework [GW06] employed in our work allows for an online update of material attributes, in particular the per-element elastic modulus, which affects the reaction to forces. Fast breast deformation simulation is thereby for the first time amenable to improve accuracy and confidence of breast surgeons compared to the de-facto standard techniques for localization of target structures.

1 Problem Statement and Prior Art

Real-world materials exhibit non-linear reactions to stress: when a certain stress level is exceeded, they react with a non-linear change of stiffness. In contrast, linear material properties in isotropic materials following Hooke's law are not capable to reflect this property. Our goal is to implement a simplified isotropic non-linear material law by adapting the per-element elastic modulus in every simulation step. Specifically, we adapt this method to simulate plausible breast deformations, which can be mimicked by a relatively soft base elastic modulus in combination with a stiffening of the elements under load. Other work tried to achieve similar objectives by employing more advanced non-linear material laws. However, they will not be capable of real-time simulations, though they model the physical world more convincingly. For a clinical setting, a compromise has to be found between fast calculations and sufficiently realistic material behavior which we believe we have achieved for the first time with the approach presented.

Previous work tried to match prone and supine breast shapes by employing finite element analysis using non-linear material laws [RNHN08]. However, the computational complexity of this approach is high and the setup of the model difficult to be performed in time-critical clinical routine. The fastest available implementations of dynamic non-linear models [HHM+11, TCO08] are based on explicit finite element approaches, which limit the largest possible time step in a dynamic simulation. Furthermore, in this case the defor-

erschienen im Tagungsband der INFORMATIK 2011
Lecture Notes in Informatics, Band P192
ISBN 978-3-88579-286-4

mation simulation has to be followed by a non-rigid registration step to achieve the final results, which might decrease utility and certainly speed.

In our work, we evaluate the performance of three stress norms controlled by two different approaches that dampen the oscillations caused by the explicit dynamic update of the per-element elastic modulus.

2 Material and Methods

Standard breast MRI data was obtained from five volunteers[1], once in prone (facing down) and once in supine (facing up) position. All datasets were segmented into rigid and deformable tissue using a semi-automatic tool [WFFH11], where the breast parenchyma and the fatty tissue was considered elastic, while the thorax and muscular tissue were considered as Dirichlet boundary conditions. A volumetric tetrahedral mesh was generated from a downsampled version of this data. The finite element method used to simulate the deformation of the breasts is based on the co-rotated Cauchy strain formulation [GW08]. The novel aspect of our work is the update of the per-element stiffness based on the stress it experiences in a given simulation step. We have implemented different stress tensor norms to evaluate their suitability for the task, namely one based on the eigenvalues of the stress tensor that can take into account the directionality of the principal stress, one based on the trace of the tensor, and the von Mises stress tensor norm [Bat02]. The stiffness is then adjusted per element and time step, according to the stress it encounters. Custom visualization methods allow to view the deformation along with characteristic attributes like, e.g., the principal stress directions and the von Mises norm.

Since no prior work has approached the modeling of tissue stiffness with the described approach, numerous variants of the real-time stiffness update have been implemented to evaluate and compare their characteristics and performance. For better comparability, a simple and regular mesh has been set up, consisting of a ground plate and a soft box on top of it that has an adjustable size and number of finite elements (tetrahedra) and can thus be used to study microscopic effects on single elements, or macroscopic effects on a larger scale. The box has material parameters that are used for the breast model as well, i.e. a Poisson ratio (the ratio of transverse to axial strain of a stretched/compressed material; cf. Fig. 1) of 0.43 and a base stiffness of 1 kPa. In the tests, the gravity direction and strength was used to cause controlled deformations.

The von Mises stress tensor norm (cf. Eqn. 1; [Bat02]) takes into account all elements of the raw stress tensor to calculate a scalar metric of the stress. It has been implemented to serve as a reference standard, since it is a well-established stress norm

$$||\sigma||_{\text{Mises}} = \sqrt{3\sum_{k=4}^{6}\sigma_k^2 + \frac{3}{2}\sum_{k=1}^{3}(\sigma_k - \bar{\sigma})^2}. \quad (1)$$

[1] Bilateral images, except dataset ID 4.

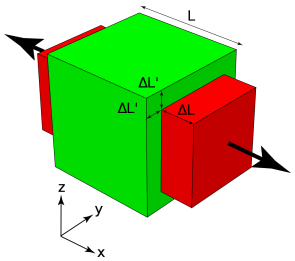

Figure 1: Assuming tension along x, a first-order approximation of the Poisson ratio ν of a linearly elastic material is $\nu = \frac{\Delta L'}{\Delta L}$. The definition, however, is in terms of strain: $\nu = -\frac{d\varepsilon_{\text{trans}}}{d\varepsilon_{\text{axial}}}$

In this contribution, we first propose a stress norm taking the relation of the first and second plus third eigenvalues of the stress tensor into account, weighted by a factor. This is based on the idea that the stiffening of the material should occur mostly when the stress is large in one direction. The eigenvectors of the stress tensor describe the principal stresses, i.e. the direction of the plane orthogonal to which the largest stress occurs, and the eigenvalues the stress magnitude in the respective direction. With $|\lambda_0| > |\lambda_1| > |\lambda_2|$ the eigenvalues of the stress tensor, the relative element stiffness $||\sigma||_{\text{r}}$ was set to

$$||\sigma||_{\text{r}} = \alpha\lambda_0, \tag{2}$$

if $|\lambda_0| > \gamma(|\lambda_2| + |\lambda_3|)$. The factor γ determines the level of anisotropy the stress of the element should exhibit. For low values, stress in the form of pressure or tension from all directions causes similarly high stiffness updates as for unidirectional pressure or tension, while this does not hold for high values of γ.

Second, the trace of the stress tensor $\lambda_0 + \lambda_1 + \lambda_2)$ is an alternative scalar norm of the stress tensor that is easy to implement and fast to calculate, and also cited as a measure of gross stress.

From the chosen stress tensor norm, a stiffness update has to be derived. Here, the initial hypothesis was that real-world materials behave non-linear under compression, e.g., the stiffness increases exponentially when the stress grows. The first implementation thus raised $||\sigma||$ to some user defined power. The oscillations for the first time observed visually in this stiffness update model led to the development of a stiffness update damping mechanism.

Initially, for all metrics an absolute update mode had been implemented. In the absolute update mode, the relative stiffness is set to $s_{\text{r}} = 1 + \alpha \cdot ||\sigma||$ with α a user-defined factor, and $||\sigma||$ the chosen stress norm. This might lead to oscillations, eventually only after considerable time, because the explicit updates of the per-element elastic modulus (stiffness) in the simulation steps increases the stored elastic energy in the linear elastic model and thus affects the stability of the approach. In other words, the internal forces in the body are mainly proportional to the elastic modulus, and thus updating this value while keeping the deformation causes higher elastic energy. Therefore, we propose to use a dynamic simulation model exhibiting damping and inertia and to update the elastic modulus in small

steps, which is accomplished by an automatically set stiffness damping coefficient.

First, a time-dependent damping factor $\omega(t)$ has been designed that decreases from 1 to 0, and is use to calculate the new stiffness. Let $s_{\mathrm{r}}(t)$ be the relative stiffness value calculated from the stress measure at time t, and $s_{\mathrm{r}}(t-1)$ be the previous value that was set for the element. The new value is then not taken directly, but adapted to be

$$s_{\mathrm{r}}(t) = (1-\omega(t))s_{\mathrm{r}}(t-1) + \omega(t)s_{\mathrm{r}}(t). \tag{3}$$

For the time-dependent damping factor $\omega(t)$, different functions have been tested. Exponential damping is often encountered in nature, thus we implemented $\omega(t) = e^{-\alpha\pi t^2}$. In addition, a simplified damping that is easily scaled to be 0 for any value $t_0 > 0$ is given by

$$\omega(t) = \frac{\left(\cos\left(\frac{\pi t}{t_0}\right)+1\right)}{2}. \tag{4}$$

Second, a damping factor proportional to the average per-element stress change has been implemented. The advantage is that no maximum time t_0 has to be set at which the stiffness update stops, but rather the speed of update is proportional to the average stiffness change in the elements. This method has proven to be superior to all others, as will be explained in the results section 3.

Next, a test application was designed to examine the per-element reaction on stress over time. In this application, it is possible to set start and end values for different parameters, and to increase/decrease these parameters during simulation. This is intended to avoid abrupt jumps in external forces et Cetera. The application then carries out one or more simulation steps, records the state of the elements, varies the parameters, and starts over. From this, we obtain a time curve of the state of all elements during the simulation. The most important parameter that can be recorded is the relative per-element stiffness resulting from the described stiffness update, since this parameter directly relates to the series of stiffness updates. Further details and explanations will be provided in the results section below.

3 Results

The stress norms have been evaluated on an artificial dataset prior to the application on breast MRI data to adjust the parameters to reasonable values. In these experiments, it has become obvious that the scalar von Mises stress norm is more robust than the directional eigenvalue based norm, in which the largest eigenvalue is related to the sum of the other two eigenvalues. The stress tensor trace figured out to be unsuitable for the task.

As described before, several metrics based on the elements and vertices have been implemented to update the per-element relative stiffness in each simulation step. The quantitative evaluation of the obtained deformation on a larger set of volunteer data from MRI is

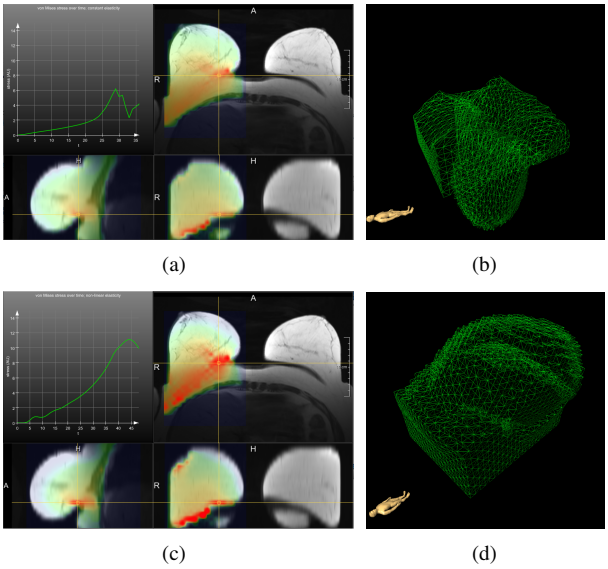

Figure 2: (a) Orthogonal slices through the breast volume from which the FE model was generated, with a color overlay indicating the stress (according to the von Mises norm) that the elements are experiencing. In this Fig., no stiffness update is applied to the elements. The graph shows a plot of the von Mises stress over a number of simulation steps for the voxel indicated by the crosshair. Note the peak at the 29^{th} simulation step, where the deformed mesh begins to exhibit physically implausible behavior (b). (c) Same model with stiffness update. The stress the elements can take with the stiffness adapted to the von Mises stress saturates on an almost doubled level and at a later simulation step, while a physically realistic and stable deformation is obtained when for example simulating the supine positioning of a patient during surgery using a FE model derived from an MRI acquired in prone positioning (d).

ongoing. Instead, for this work the described phantom was employed to develop and characterize the algorithms, which are then applied to volunteer data and qualitatively assessed and measured in terms of performance.

3.1 Phantom Experiments

In the phantom experiments, it has become obvious that the scalar von Mises stress norm is more robust than the directional eigenvalue based norm, in which the largest eigenvalue is related to the sum of the other two eigenvalues. The stress tensor trace figured out to be unsuitable for the task. Still, while the results with the von Mises stress norm and the eigenvalue-based stress measure looked promising visually, more or less pronounced oscillations were observed after longer simulation runs and have been addressed with the damping mechanisms described above.

The time-dependent update damping shown in Eqn. (4) appeared to be satisfactory at

first with t_0 set to any durations that allowed for 20-40 simulation steps. Macroscopically the deformed mesh came to rest. Looking at the stress field revealed slightest changes to the stiffness, however, and continuing the simulation without damping eventually led to increasing oscillations and finally instability of the simulation.

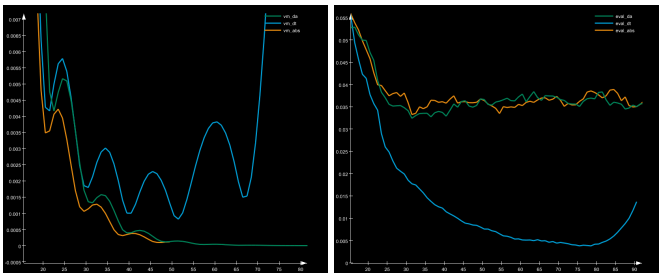

(a) (b)

Figure 3: A comparison of curves that show the average per element relative stiffness update, which correlates with the overall stress the mesh experiences. The four plots each show the three curves for the three update mechnisms, absolute (orange), time-damped (blue), and adaptively damped (green). (a) von Mises stress; (b) eigenvalue criterion. Note that the curves for the time-damped update (blue) start increasing after an intermediate stability period, which was visually complemented either with a break-down of the mesh or beginning oscillations.

The most robust damping method implements a continuous update proportional to the average element stress change. Fig. 5 illustrates the outcomes of the simulation after comparable simulation durations. Since the ill effects of insufficient damping might occur a long time after superficially the simulation appears to be stable, we tested this damping scheme for much longer periods of time; however, we could not observe any oscillations with this scheme in all of our tests.

Curves were plotted to track the average update of relative stiffness from simulation step to simulation step for all combinations of update mechanisms (absolute – abs; time-damped – dt; adaptively damped – da) and stress norms (von Mises – vm; eigenvalues – eval). Figure 3 shows plots underlining how the proposed adaptive damping mechanism is superior to a time-dependent damping which would not prevent the mesh from breaking after the damping period. It is notable also that the adaptive damping brings a slight lag into the curve. Not seen on these plots is the behavior of the curves without damping after a long simulation, when the stress will start to increase again and cause new oscillation. This is never experienced with the adaptive damping method.

Also, from the same figure it is obvious that the von-Mises criterion has oscillations (Fig. 3(a)), and that the eigenvalue based stress criterion is very unstable (Fig. 3(b)). Further experiments have been conducted to assess the stiffness update for the tetrahedral mesh in order to explain the oscillations described before.

We have observed checkerboard-like patterns in the relative stiffness maps in the artificial phantom. Fig. 4 illustrates this. The stress norm jumps in magnitude from one element to its neighbor, possibly causing an ill-posed system matrix that causes numerically inaccuracies. Consequently, oscillations and break-down of the mesh might be the result,

ISBN 978-3-88579-286-4

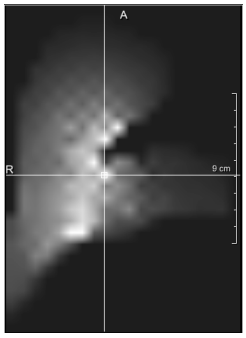

Figure 4: Illustration of a problem encountered with the adaptive stiffness update damping based on tetrahedral meshes with the von-Mises stress norm determining the stiffness update. Note the checkerboard-like intensity value jumps between neighboring voxels. The color values correspond to the relative stiffnesses of the central of the five tetrahedrons forming one voxel.

conforming with the observations. A simplified phantom consisting of only eight voxels, equaling to 40 tetrahedrons, allowed us to compare the different metrics. For this experiment, the visualization of the relative stiffness was adapted to oversample the original voxels with a factor of 10 to visualize individual tetrahedrons.

3.2 Patient Data and Performance

We have measured the performance of the implementation on volunteer datasets sampled to $5 \times 5 \times 5$ mm resolution, yielding varying numbers of elements (cf. Table 3.2). The resolution can be reduced to $10 \times 10 \times 10$ mm to increase speed by almost an order of magnitude. For the practical application, only the simulation of either the left or the right breast is required; a restriction of the field of view to this area would also double the speed. Note that all measurements were taken for only stress norm based on the eigenvalues and the adaptive damping, since this is the computationally most expensive combination. Note that for the von-Mises stress norm instead of the eigenvalue-based norm, the update times in Table 3.2 can be divided by three, resulting in an overall faster simulation.

Applied to breast data, we are now able to realistically simulate gravity of a model using a base elastic modulus of 1 kPa. The results with and without the stiffness update are compared in Fig. 2. Especially, for one single voxel, we plot the von-Mises stress norm over the time. Note that the color map and graph scale are the same in the top and bottom row of the figure.

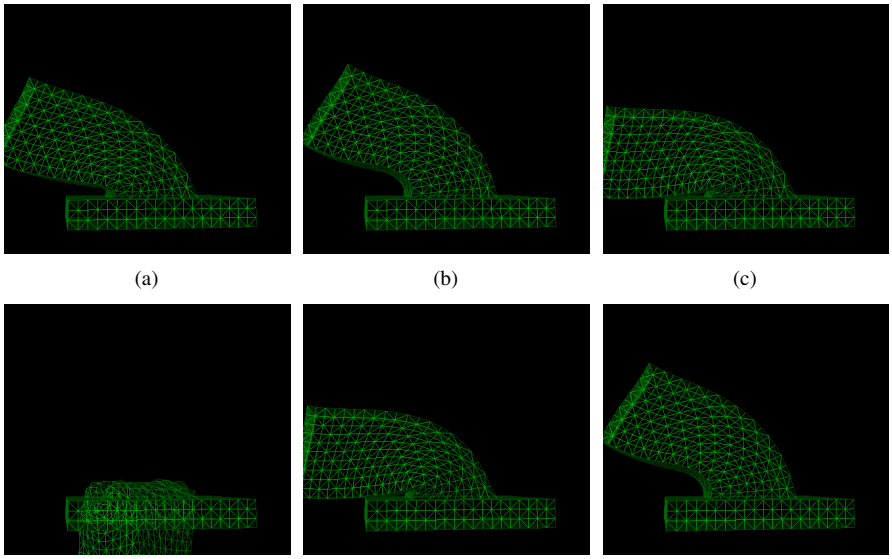

Figure 5: A comparison of the influence of different stiffness update mechanisms on different stiffness measures. Per row, one stress norm is used, and per column, one update mechanism applies. ROWS: von Mises stress; eigenvalue weights; COLUMNS: absolute update; time-damped update; adaptive damping update. The simulations were parameterized to yield the maximum possible bend without rupture in absolute update mode.

4 Conclusion and Further Work

Physically plausible breast deformations can be handled with our fast framework. It is particularly beneficial for practical applicability that only a single parameter has to be adjusted, and that the behavior of the simulation is very robust against variations in the choice of the parameter.

Further work is currently being performed to replace the stress tensor norms with purely geometric measures that reflect the element's stretch or compression, which might show a better behavior in terms of the size of the possible update steps.

Finally, we aim at an integration of these works into a system that matches an MRI scan take pre-interventionally to a body surface scan taken with the patient placed on the surgery table. We wish to examine the accuracy obtained with an approach like this compared to the conventional target area delineation using metal wire guides.

References

[Bat02] Klaus-Jürgen Bathe. *Finite Element Procedures*. Prentice Hall, 2002.

Table 1: Timing statistics. 25 simulation time steps (sim.) were performed, and the same number of per-element stiffness update operations (up.). Timings were measured on an Intel Core i7 Quad 3.0GHz CPU.

ID	#ele.	time sim. [ms]	time up. [ms]	total 25 steps [sec]
4	47,895	189	48	5.9
2	99,390	400	98	12.5
0	158,340	644	149	19.8
3	158,340	628	149	19.4
1	313,335	1432	318	43.8

[GW06] Joachim Georgii and Rüdiger Westermann. A Multigrid Framework for Real-Time Simulation of Deformable Bodies. *Computer & Graphics*, 30:408–415, 2006.

[GW08] Joachim Georgii and Rüdiger Westermann. Corotated Finite Elements Made Fast and Stable. In *Proceedings of the 5th Workshop On Virtual Reality Interaction and Physical Simulation*, pages 11–19, 2008.

[HHM+11] Lianghao Han, John Hipwell, Thomy Mertzanidou, Tim Carter, Marc Modat, Sebastien Ourselin, and David Hawkes. A hybrid FEM-based method for aligning prone and supine images for image guided breast surgery. *ISBI 2011*, pages 1239–1242, 2011.

[RNHN08] Vijay Rajagopal, Martyn P Nash, Ralph P Highnam, and Poul M Nielsen. The Breast Biomechanics Reference State for Multi-modal Image Analysis. In *IWDM '08: Proceedings of the 9th international workshop on Digital Mammography*. Springer-Verlag, 2008.

[TCO08] Z A Taylor, M Cheng, and S Ourselin. High-Speed Nonlinear Finite Element Analysis for Surgical Simulation Using Graphics Processing Units. *IEEE transactions on medical imaging*, 27(5):650–663, 2008.

[WFFH11] L Wang, K Filippatos, O Friman, and HK Hahn. Fully automated segmentation of the pectoralis muscle boundary in breast MR images. In *SPIE Medical Imaging, Computer-Aided Diagnosis*, volume 7963, 2011.

ISBN 978-3-88579-286-4